



Published in final edited form as:

Cancer Res. 2011 May 15; 71(10): 3649–3657. doi:10.1158/0008-5472.CAN-10-3623.

Contribution of Abcc10 (Mrp7) to *in vivo* paclitaxel resistance as assessed in *Abcc10*^{-/-} mice

Elizabeth A. Hopper-Borge^{1,*}, Timothy Churchill¹, Chelsy Paulose¹, Emmanuelle Nicolas³, Joely D. Jacobs¹, Olivia Ngo¹, Yehong Kuang^{4,5}, Alex Grinberg⁶, Heiner Westphal⁶, Zhe-Sheng Chen⁴, Andres J. Klein-Szanto⁷, Martin G. Belinsky¹, and Gary D. Kruh²

¹Program in Developmental Therapeutics, Fox Chase Cancer Center, Philadelphia, PA. 19111

²University of Illinois at Chicago, Department of Medicine, and Cancer Center, Chicago, IL 60612

³Genomics Facility, Fox Chase Cancer Center, Philadelphia, PA 19111

⁴St John's University, College of Pharmacy and Allied Health Professionals, Department of Pharmaceutical Sciences, Jamaica, New York, NY, 11439

⁵Department of Dermatology, Xiang Ya Hospital, Central South University, Changsha, China

⁶National Institute of Child Health and Human Development, National Institutes of Health, Bethesda, Maryland 20847

⁷Department of Pathology, Fox Chase Cancer Center, Philadelphia, PA 19111

Abstract

Recently we reported that the ATP-binding cassette transporter Abcc10, also known as multidrug resistance protein 7 (Mrp7), is able to confer resistance to a variety of anticancer agents including taxanes. However, the *in vivo* functions of the pump have not been determined to any extent. Here we generated and analyzed *Abcc10*^{-/-} mice in order to investigate the ability of Abcc10 to function as an endogenous resistance factor. Mouse embryo fibroblasts derived from *Abcc10*^{-/-} mice were hypersensitive to docetaxel, paclitaxel, vincristine and Ara-C and exhibited increased cellular drug accumulation, relative to wild type controls. *Abcc10* null mice treated with paclitaxel exhibited increased lethality associated with neutropenia and marked bone marrow toxicity. Toxicity in spleen and thymus was also evident. These findings indicate that Abcc10 is dispensable for health and viability, and that it is an endogenous resistance factor for taxanes, other natural product agents and nucleoside analogs. This is the first demonstration that an ATP-binding cassette transporter other than P-glycoprotein can affect *in vivo* tissue sensitivity towards taxanes.

Keywords

Drug transport; drug resistance; Mrp7; Abcc10; taxanes; paclitaxel

Introduction

Paclitaxel and its semi-synthetic analogue, docetaxel, have established roles in the treatment of common cancers such as breast, lung and prostate, as well as other less common tumors such as ovary and head and neck (1). Taxanes exert cytotoxicity by stabilizing microtubules

*To whom correspondence should be addressed: Elizabeth Hopper-Borge, Fox Chase Cancer Center, 333 Cottman Avenue, Philadelphia, PA. 19111, Phone: 215-214-1505, Fax: 215-728-3616, EA_Hopper@fccc.edu.

and inducing cell cycle arrest. Because of the clinical utility of taxanes, cellular factors that affect sensitivity have been extensively investigated. Several mechanisms of resistance have been identified using cellular models of acquired taxane resistance, including increased expression of the P-glycoprotein drug efflux pump, acquired mutations in tubulin, increased expression of specific tubulin isoforms and alterations in signaling pathways involved in tubulin function (2, 3). Correlative clinical studies have largely highlighted the importance of two of these mechanisms - increased expression of P-glycoprotein and of the class III beta tubulin (4–8).

Recently we determined that ABCC10 (MRP7), a member of the MRP family of drug efflux pumps, is a novel cellular resistance factor for taxanes (9–13). Analysis of the drug resistance capabilities of ABCC10 in stably transfected HEK293 cells revealed that it is unique among MRPs in that taxanes are a prominent feature of its resistance profile (12). In addition, ABCC10 is able to confer resistance to another class of microtubule active agents - vinca alkaloids - and to certain nucleoside analogs (13). Ectopic expression of the pump in highly drug sensitive *Mrp1^{-/-}/Mdr1a/b^{-/-}* (*Abcc1*, *Abcb1a/Abcb1b*) fibroblasts confirmed the facility of ABCC10 for conferring resistance to taxanes and vincristine, and in addition uncovered its activity towards a range of other natural product agents including daunorubicin, etoposide and SN-38 (13). Insights into the substrate selectivity of ABCC10 have been afforded by *in vitro* transport studies. In addition to largely hydrophobic molecules such as natural product anticancer drugs, ABCC10 is able to transport amphipathic anions, as is the case for other MRPs (10). Among a number of organic anions previously identified as transport substrates of other MRPs, the selectivity of ABCC10 appears to be restricted to glucuronides such as E₂17βG, with additional modest activity towards the glutathione conjugate LTC₄ (14).

While these studies provided insights into the *in vitro* properties of ABCC10 as assessed in transfected cell lines and transport assays and suggest that ABCC10 could play a role in sensitivity towards taxanes, little is currently known about the *in vivo* functions of the pump. To gain insights into the physiological and pharmacological functions of ABCC10, and in particular to determine its contribution to inherent sensitivity towards taxanes, an *Abcc10^{-/-}* mouse was generated and analyzed. Here, it is shown that *Abcc10^{-/-}* mice are sensitized to paclitaxel and that cell lines derived from this mouse model are hypersensitive to this agent, other natural product agents and Ara-C. We conclude that *Abcc10* is dispensable for health and viability and that it contributes to the intrinsic resistance of cells and tissues towards several commonly employed chemotherapeutic agents, including taxanes.

Material and Methods

Targeted disruption of the *Abcc10* gene and generation of *Abcc10^{-/-}* mice

A mouse strain 129-derived lambda phage genomic library was probed with a 389-bp fragment containing the 5' end of the *Abcc10* coding sequence, and a ~12-kb *Abcc10* clone was isolated. Nucleotide sequence analysis (ABI 377 DNA sequencer; Applied Biosystems, Foster City, CA) indicated that the clone encompassed exons 6–16 (amino acids 204–410) of the *Abcc10* gene, corresponding to nucleotides 612–231 of the coding sequence. The left and right arms of a targeting vector were excised and inserted, respectively, into the 5' and 3' cloning sites of the pgk-neo cassette of the PNT plasmid (15). The resulting vector was designed to delete exons 6 – 8, encoding amino acids 204–332 (nucleotides 612–996). As a result, the Walker B motif required for nucleotide binding is deleted and a frame-shift is introduced in the coding sequence.

The nucleotide sequence of the cloned arms was confirmed, and the ~5.4 kb targeting vector was linearized with NotI. The vector was electroporated into strain 129-derived R1

embryonic stem cells, and individual colonies isolated after positive/negative selection with G418 and gancyclovir (15). EcoR1-digested genomic DNA was prepared and analyzed for proper right arm recombination by Southern blot analysis using a 3' probe. A PCR strategy was used to identify correct left arm recombinants. The primers were 5' CCT TTT GCC CCA CAT CTC AACC 3' (*Abcc10* sequence), and 5' CGAGGGCCCCTGCAGGTC 3' (vector sequence). The absence of randomly integrated vector sequences was confirmed by Southern blot analysis using a neomycin probe. Prior to injection into blastocysts, left arm recombination was confirmed by Southern blot analysis.

Two correctly targeted ES clones were injected into C57BL/6J blastocysts, and the blastocysts were implanted in pseudopregnant females. Male chimeric progeny were crossed with female C57BL/6J (in-house-bred) mice. Germ-line transmission of the targeted allele was confirmed by Southern blot analysis, as described above for the right arm, and for the left arm by PCR using: 5'-GTCCAACCTTTTGCCCCACATCT-3' and 5'-AATTGACCTGCAGGGGCCCTCG-3', which generates a ~3.5 Kb band. Subsequent genotyping was accomplished by PCR analysis of tail DNA using a single tube 3-primer reaction with: 5'-CCTGCCTGCTGGAGACCAG-3', 5'-CCCAGGTGTCAAGGCAACTG-3', and 5'-AATTGACCTGCAGGGGCCCTC-3'. The first two primers generate a 400-bp wild-type product, and the latter pair generate a 200-bp product from the targeted allele. As experiments proceeded using mixed strain mouse (C57BL/6J × 129) knock out mice, the *Abcc10* null allele was backcrossed for eight generations onto the C57BL/6J background.

Antibody preparation and immunoblot analysis

A cDNA fragment encoding amino acids 1443 – 1491 of *Abcc10* was inserted into pGEX-T (Amersham Biosciences, Piscataway, NJ) and the resulting glutathione S-transferase fusion protein was purified using glutathione beads according to the manufacturer's recommendations. Rabbits were immunized with the purified recombinant protein and the specificity of the resulting antiserum was confirmed on membranes prepared from ABCC10 baculovirus-infected cells. *Abcc10* was detected in kidney cells and spleen tissue using polyclonal antibody (1:5000) and an alkaline phosphatase-conjugated secondary antibody (1:30,000). ABCC10 antibody (P18, Santa Cruz Biotechnology, Santa Cruz, CA) (1:200) and an alkaline phosphatase-conjugated secondary antibody (1:2000) was used for the mouse embryo fibroblast immunoblot. Total cellular lysates prepared from cultured cells and spleen membrane fractions were subjected to SDS-polyacrylamide gel electrophoresis and proteins were electrotransferred to nitrocellulose filters. All blots were incubated with antibodies using the Millipore Snap ID system. β -Actin antibody (Cell Signaling Technology, Danvers, MA) was used at a concentration of 1:5000.

Cell line preparation and cellular assays

To prepare mouse embryo fibroblasts mice (C57BL/6J × 129 and C57BL/6J) were set up in timed matings and at day 13–14 embryos were harvested. Embryos were minced, aspirated through a 1 mL syringe and incubated in 0.25% trypsin for 15 min in a 37°C incubator. The cells were spun down at 1000 rpm for 5 min and cell pellets were resuspended in 10% DMEM and plated into flasks. Confluent cells were transfected with a plasmid containing SV40 T antigen and a blasticidin resistance marker to select for immortal lines, as previously described (16). Genetic veracity of mouse embryo fibroblasts was verified by the Fox Chase Cancer Center Biomarker and Genotyping facility every two months, and upon defrosting new vials, using genotyping and/or qRT-PCR. Drug accumulation and cellular proliferation assays were performed as previously described (13, 17, 18). Vincristine, paclitaxel, and cytarabine (Ara-C) were purchased from Sigma Chemical Company (St. Louis, MO). [³H] paclitaxel was purchased from Moravek (Brea, CA).

Kidney cell line preparation

Kidneys isolated from wild-type and knock out mice were finely minced and placed into 10 mL of 0.02% collagenase and incubated for 2 h at 37°C. The cells were washed four times with serum free DMEM and then transferred to 1.6 mL of low calcium DMEM supplemented with 5% horse serum in a swine gelatin coated flask (19). The next day, the supernatant was removed and free floating cells were transferred to another flask. The resulting primary cultures were expanded and used for immunoblot analysis.

Sensitivity of mice to paclitaxel

For survival curves, wild-type and knock-out mice (C57/BL6x129) were administered various concentrations of paclitaxel as a single intraperitoneal injection and monitored for morbidity. For experiments in which white blood cell counts and body weight were analyzed, mice were administered a single 20 mg/kg intraperitoneal injection of paclitaxel and measurements of white blood cell counts and body weight were made daily for 6 days. Blood samples were obtained by orbital bleeding and white blood cells were isolated using Zap-Oglobin II (Beckman, Brea, CA) according to the manufacturer's instructions. White blood cell counts were analyzed using a Coulter Z1 series particle counter (Beckman Coulter, Miami, FL). Paclitaxel (LC Laboratories, Woburn, MA) was dissolved in methanol at a concentration of 50 mg/mL and filter sterilized.

Animal handling, blood chemistries and hematology

Animals were maintained in the Fox Chase Cancer Center laboratory animal facility and housed in a temperature- and humidity-controlled environment under 12h light/dark cycles. Mice were fed a standard rodent diet (Lab Diet 5013, PMI Nutrition, Brentwood, MO) and had free access to water. The Fox Chase Institutional Animal Care and Use Committee approved the protocol. Peripheral blood was obtained by orbital bleeding. Blood chemistry and hematologic variables were determined at Antech Diagnostics (Farmingdale, NY).

Analysis of *Abcc10* RNA expression in mouse tissues

Total RNA was isolated from various mouse tissues using the RNeasy mini kit (Qiagen, Valencia, CA) according to the manufacturer's suggestions. RNA was reverse-transcribed using the M-MLV reverse transcriptase and a mixture of anchored oligo-dT primers and random decamers. Aliquots of cDNA were used for qRT-PCR. The sequences of the primers were: GGGCAATTGGTCCGAACA, CTTGTTTCCTTCTCAGCCCAGG and probe 6FAM-TGAGATCCTGCCGCTGGTACAAGCTG-BHQ1PCR master mix (Applied Biosystems, Foster City, CA) were used. Cycling conditions were 95°C, 15 min followed by 40 cycles (95°C, 15 sec; 60°C, 60 sec). A 5 points 4-fold dilutions standard curve was used to convert the Ct values into quantities. To compare transporter expression levels we normalized all mean quantity data to an independent gene *Ppib* (cyclophilin B). For these assays, two wild-type and two *Abcc10*^{-/-} samples were examined for spleen, and thymus. Further, two independent measurements were taken for each sample.

Histopathological analysis

Tissues were fixed in 10% phosphate-buffered formalin, embedded in paraffin, sectioned, and stained with hematoxylin/eosin.

RESULTS

Generation of *Abcc10*^{-/-} mice

To examine the *in vivo* functions of *Abcc10*, an *Abcc10*-null mouse was generated by homologous recombination in ES cells. The vector targeted amino acids 204–410 of the

protein, which harbor most of nucleotide binding domain 1 including the entire Walker B motif (Figure 1A). Southern blot (Figure 1B) and PCR analysis (not shown) confirmed correct recombination, and *Abcc10*^{-/-} mice were derived. Analysis of *Abcc10* transcript expression in mouse tissues revealed a wide distribution pattern, with highest levels in testes, bladder, kidney and ovary (Figure 1C). Based upon the high levels of *Abcc10* transcript in kidney, this tissue was analyzed to evaluate loss of *Abcc10* protein in *Abcc10*^{-/-} mice. *Abcc10* protein was readily detected in primary kidney cells lines isolated from wild type mice but was undetectable in kidney and spleen cells isolated from *Abcc10* null mice, confirming the absence of *Abcc10* protein in the knockout mice (Figure 1D). Loss of *Abcc10* protein was also confirmed in spleen. *Abcc10*-null mice appeared normal with respect to appearance, behavior and fertility. Analysis of a panel of hematopoietic and blood chemistry parameters (Supplemental Table 1), and histopathological analysis of tissues, did not reveal significant differences between wild-type and *Abcc10* null mice.

***Abcc10*^{-/-} mouse embryo fibroblasts are hypersensitive to natural product agents and Ara-C**

Mouse embryo fibroblast (MEF) cell lines were generated from *Abcc10*-null and wild type mice as a cellular model to study the protective function of *Abcc10*. Immunoblot analysis confirmed the presence of *Abcc10* protein in wild-type MEFs but not in MEFs derived from *Abcc10* knockout mice (Figure 2A). The cell lines were analyzed for sensitivity towards representative anticancer agents that we previously determined were components of the human ABCB10 drug resistance profile - paclitaxel, docetaxel, vincristine and Ara-C (12, 13). *Abcc10*^{-/-} MEFs were hypersensitive to each of these agents (Figure 2B). The highest levels of hypersensitivity were observed towards docetaxel, for which *Abcc10*^{-/-} MEFs were 22.2-fold more sensitive than wild-type MEFs (IC₅₀ values of 0.59 ± 0.22 nM vs. 13.1 ± 3.8 nM, for *Abcc10*^{-/-} and wild type MEFs, respectively; *P* = 0.031). For paclitaxel, vincristine and Ara-C, *Abcc10*^{-/-} MEFs were 4.2, 2.3 and 3.9-fold more sensitive than wild-type MEFs (respective IC₅₀ values of 55.1 ± 9.1, 29.2 ± 5.3 and 48.9 ± 10 nM for *Abcc10*^{-/-} MEFs versus 229 ± 0.3, 66.0 ± 15, and 191 ± 27 nM for wild type MEFs; *P* = 0.004, 0.031 and 0.008, respectively).

The impact of genetic deficiency of *Abcc10* was also evaluated in the context of MEFs isolated from *Abcc10*^{-/-} mice that had been backcrossed to C57BL/6 (Figure 2C). A similar pattern of hypersensitivity was observed for this genetic background, with *Abcc10*^{-/-} MEFs exhibiting 2.7, 1.2 and 3.9-fold increased sensitivity compared to wild-type MEFs (respective IC₅₀ values of 229 ± 27, 258 ± 12 and 501 ± 130 μM for *Abcc10*^{-/-} MEFs versus 83.9 ± 20, 219 ± 5.6 and 127 ± 22.3 nM for wild type MEFs; *P* = 0.0005, 0.016 and 0.016, respectively).

To confirm that the increased sensitivity of *Abcc10*-null MEFs was attributable to genetic deficiency of a drug efflux pump rather than secondary changes that might arise as a consequence of the *Abcc10*^{-/-} lesion, the cellular kinetics of paclitaxel accumulation and efflux were analyzed (Figure 2D). As expected, accumulation of paclitaxel in *Abcc10*^{-/-} MEFs was significantly greater than in wild-type cells, regardless of the background strain from which the MEFs were derived. Following a 30 min incubation in 0.1 μM [³H]paclitaxel, accumulation in *Abcc10*^{-/-} MEFs was increased 44% and 63% respectively, in C57BL/6x129 and C57BL/6 *Abcc10*^{-/-} fibroblasts, compared to their respective control cell lines (*P*=0.002 and .002, respectively). The accumulation deficit for paclitaxel was greater for genetic deficiency of *Abcc10* in MEFs on the mixed genetic background compared to the C57BL/6 background, in close concordance with the higher levels of paclitaxel sensitization observed for *Abcc10*^{-/-} MEFs on the mixed versus C57BL/6 background (Figures 2). Representative dose response curves for docetaxel, paclitaxel, vincristine and Ara-C using *Abcc10*^{-/-} and wild-type MEFs derived from the C57BL/6J ×

129 strain are shown in Figure 3(A–D). Increased sensitivity was observed for *Abcc10*^{-/-} MEFs compared to wild-type MEFs for paclitaxel (Figure 3A), docetaxel (Figure 3B), vincristine (Figure 3C) and Ara-C (Figure 3D).

***Abcc10*^{-/-} mice are hypersensitive to paclitaxel**

Having determined in the above *in vitro* experiments that genetic deficiency of *Abcc10* confers cellular sensitivity to a range of agents including taxanes, the *in vivo* pharmacological functions of *Abcc10* were investigated next by challenging *Abcc10*^{-/-} and wild-type mice with paclitaxel. Sensitivity to paclitaxel was markedly increased in *Abcc10*^{-/-} mice, as indicated by the striking separation of the dose-response curves (Figure 4A). The minimal toxic dose for *Abcc10*^{-/-} mice was 32 mg/kg compared to 150 mg/kg for wild-type mice, or ~ 5-fold lower than that of wild-type mice. Only 33% of the *Abcc10*^{-/-} mice survived at 160 mg/kg, whereas 10% of wild-type mice survived at this dose. At 250 mg/kg 100% of *Abcc10*^{-/-} mice died, whereas 80% of wild-type mice survived.

Body weight and white blood cell counts were analyzed in mice challenged with paclitaxel (Figure 4, B and C). Although the intention in this experiment was to select a dosage that was sublethal (20 mg/kg), significant morbidity was observed. Presumably, this was attributable to stress associated with daily orbital bleeds. Nevertheless, the increased sensitivity of *Abcc10*^{-/-} mice towards paclitaxel was reflected in both body weight and white blood cell parameters. Wild-type mice lost no more than 10% of body weight and eventually recovered, whereas *Abcc10*^{-/-} mice lost up to 20% of body weight. In wild-type mice, depression of white blood cell counts was not observed, whereas in *Abcc10*^{-/-} mice striking reductions were apparent, with a 70% reduction observed at day 6.

***Abcc10* protects bone marrow, spleen and thymus**

Histopathologic analysis of wild-type and *Abcc10*^{-/-} mice treated with paclitaxel revealed significant changes in hematopoietic and lymphoid tissues in *Abcc10*^{-/-} mice, whereas the corresponding tissues in wild-type mice appeared little changed. Marked hypoplasia was seen in the bone marrow of *Abcc10*^{-/-} mice, whereas wild-type mice exhibited minimal or no changes (Figure 5 A). *Abcc10*-null mice had smaller spleens in which the lymphoid follicles (white pulp) were diminished in number and size (Figure 5 B). In addition, erythroid and myeloid cell populations in the red pulp were decreased and replaced by histiocytes and stromal cells. In *Abcc10*^{-/-} mice, the cortex of the thymus was decreased in size in association with lymphocyte apoptosis and/or depopulation (Figure 5 C). To gain further insight into these observations, qRT-PCR analysis of RNA isolated from spleen and thymus of *Abcc10*^{-/-} and wild-type mice was performed. *Abcb1a*, *Abcb1b*, *Abcc1*, *Abcc3*, *Abcc4*, and *Abcc5* did not show statistically significant changes in gene expression levels as a result of *Abcc10* knockdown. Further, the levels of *Abcc2*, *Abcc6*, and *Abcc9* in these tissues were too low to draw conclusions. Overall, there were no strong compensatory changes based upon *Abcc10* phenotype.

DISCUSSION

In previous studies we determined that ectopic expression of ABCC10 confers resistance to taxanes, vinca alkaloids and a range of nucleoside analogs such as Ara-C (12, 13). Of these agents taxanes were of particular interest to us because of the paucity of efflux pumps, aside from P-glycoprotein, that are established cellular resistance factors for this class of clinically important agents. Indeed, the importance of P-glycoprotein in resistance to taxanes, and the potential for ABCC10 to function as a resistance factor for this class of agents, was highlighted by the extraordinary high levels of resistance ABCC10 is able to confer to paclitaxel and docetaxel (116 and 46-fold, respectively) when it was ectopically expressed in

P-glycoprotein deficient fibroblasts (13). In view of the intriguing activities of ABCC10 in studies on transfected cells, the present study was undertaken to investigate the potential for the pump to function as an *in vivo* resistance factor.

Here it is shown by the analysis of *Abcc10*^{-/-} fibroblasts that the pump contributes to inherent cellular resistance towards each of the classes of anticancer agents that we identified in the context of transfected HEK293 cells, including the taxanes paclitaxel and docetaxel (12, 13). Importantly, the results of experiments on *Abcc10*^{-/-} MEFs, in combination with the finding that *Abcc10*^{-/-} mice are hypersensitive to paclitaxel, provide the first evidence that the pump can function as an *in vivo* resistance factor. In addition, analysis of the tissue-specific pattern of toxicity provides insights into how genetic deficiency of *Abcc10* contributes to paclitaxel hypersensitivity. Neutropenia in conjunction with marked bone marrow hypoplasia indicate that the pump affords protection against paclitaxel-induced bone marrow toxicity and suggest that reduced immunity is a significant component of morbidity in the *Abcc10*-null mice challenged with this agent. This is a noteworthy finding because bone marrow toxicity is the principal acute side effect of paclitaxel in humans. Additional insights into the contribution of *Abcc10* to *in vivo* resistance will require studies on the impact of the pump on pharmacokinetics and associated determinations of the polarity and expression of *Abcc10* in tissues involved in drug disposition.

While ABCC10 has been reported to have a wide pattern of transcript expression in human (13) and mouse tissues (present study), relatively little information is available on its expression in tumors and its susceptibility to induction under drug pressure. In a small survey involving 8 samples, ABCC10 transcript was detected in breast, lung, colon, prostate, ovary and pancreatic cancers (20). Another study described expression of ABCC10 transcript in 12 of 17 non-small cell lung cancer cell lines and reported that expression correlates with resistance of the cell lines to paclitaxel (21). With respect to inducibility, upregulation of ABCC10 transcript has been reported for a few cell lines made resistant to classes of microtubule active agents that we previously determined to be part of the pump's drug resistance profile. Upregulation of ABCC10 transcript was reported for a small cell lung cancer cell line made resistant to paclitaxel, a non-small cell lung cancer cell line with acquired resistant to vinorelbine and salivary gland adenocarcinoma cell line made resistant to vincristine (21–23). More information is needed on expression of ABCC10 in tumor samples, and in particular on tumors treated with taxanes and vinca alkaloids.

Although efflux pump inhibitors have yet to be established as a clinical strategy for sensitizing tumors to chemotherapeutic agents, the determination here that genetic deficiency of *Abcc10* is not associated with obvious health problems indicates that the normal physiological functions of the murine pump are not essential, and suggests that ABCC10 inhibitors could potentially be used in humans without side effects attributable to interference with the pump's normal functions. Several inhibitors of ABCC10 have been identified, including cepharanthine, lapatinib and nilotinib (24–26). These compounds could serve as starting points for the development of potent and selective ABCC10 inhibitors.

Supplementary Material

Refer to Web version on PubMed Central for supplementary material.

Acknowledgments

This work was supported by National Institutes of Health grants K01CA120091 to EH-B, CA073728 to GDK, 1R15CA143701 to ZSC and CA06927 to Fox Chase Cancer Center. We thank Dr. Samuel Litwin for statistical

analyses and Dr. Erica Golemis for critical comments on the manuscript. We also thank the Laboratory Animal Facility, particularly Jackie Valvardi and Simon Tarpinian, for assistance with animal maintenance.

References

1. Zelnak AB. Clinical pharmacology and use of microtubule-targeting agents in cancer therapy. *Methods Mol Med.* 2007; 137:209–234. [PubMed: 18085232]
2. Kruh GD. Ins and outs of taxanes. *Cancer Biol Ther.* 2005; 4:1030–1032. [PubMed: 16177563]
3. Orr GA, Verdier-Pinard P, McDaid H, Horwitz SB. Mechanisms of Taxol resistance related to microtubules. *Oncogene.* 2003; 22:7280–7295. [PubMed: 14576838]
4. Dumontet C, Isaac S, Souquet PJ, et al. Expression of class III beta tubulin in non-small cell lung cancer is correlated with resistance to taxane chemotherapy. *Bull Cancer.* 2005; 92:E25–E30. [PubMed: 15749640]
5. Mozzetti S, Ferlini C, Concolino P, et al. Class III beta-tubulin overexpression is a prominent mechanism of paclitaxel resistance in ovarian cancer patients. *Clin Cancer Res.* 2005; 11:298–305. [PubMed: 15671559]
6. Chiou JF, Liang JA, Hsu WH, Wang JJ, Ho ST, Kao A. Comparing the relationship of Taxol-based chemotherapy response with P-glycoprotein and lung resistance-related protein expression in non-small cell lung cancer. *Lung.* 2003; 181:267–273. [PubMed: 14705770]
7. Yeh JJ, Hsu WH, Wang JJ, Ho ST, Kao A. Predicting chemotherapy response to paclitaxel-based therapy in advanced non-small-cell lung cancer with P-glycoprotein expression. *Respiration.* 2003; 70:32–35. [PubMed: 12584388]
8. Penson RT, Oliva E, Skates SJ, et al. Expression of multidrug resistance-1 protein inversely correlates with paclitaxel response and survival in ovarian cancer patients: a study in serial samples. *Gynecol Oncol.* 2004; 93:98–106. [PubMed: 15047220]
9. Hopper E, Belinsky MG, Zeng H, Tosolini A, Testa JR, Kruh GD. Analysis of the structure and expression pattern of MRP7(ABCC10), a new member of the MRP subfamily. *Cancer Lett.* 2001; 162:181–191. [PubMed: 11146224]
10. Kruh GD, Guo Y, Hopper-Borge E, Belinsky MG, Chen ZS. ABCC10, ABCC11, and ABCC12. *Pflugers Arch.* 2007; 453:675–684. [PubMed: 16868766]
11. Kruh GD, Belinsky MG. The MRP family of drug efflux pumps. *Oncogene.* 2003; 22:7537–7552. [PubMed: 14576857]
12. Hopper-Borge E, Chen ZS, Shchaveleva I, Belinsky MG, Kruh GD. Analysis of the drug resistance profile of multidrug resistance protein 7 (ABCC10): resistance to docetaxel. *Cancer Res.* 2004; 64:4927–4930. [PubMed: 15256465]
13. Hopper-Borge E, Xu X, Shen T, Shi Z, Chen ZS, Kruh GD. Human multidrug resistance protein 7 (ABCC10) is a resistance factor for nucleoside analogues and epothilone B. *Cancer Res.* 2009; 69:178–184. [PubMed: 19118001]
14. Chen ZS, Hopper-Borge E, Belinsky MG, Shchaveleva I, Kotova E, Kruh GD. Characterization of the transport properties of human multidrug resistance protein 7 (MRP7, ABCC10). *Mol Pharmacol.* 2003; 63:351–358. [PubMed: 12527806]
15. Belinsky MG, Dawson PA, Shchaveleva I, et al. Analysis of the In Vivo Functions of MRP3. *Mol Pharmacol.* 2005
16. Johnson DR, Finch RA, Lin ZP, Zeiss CJ, Sartorelli AC. The pharmacological phenotype of combined multidrug-resistance *mdr1a/1b*- and *mrl1*-deficient mice. *Cancer Res.* 2001; 61:1469–1476. [PubMed: 11245453]
17. Kuang YH, Shen T, Chen X, et al. Lapatinib and erlotinib are potent reversal agents for MRP7(ABCC10)-mediated multidrug resistance. *Biochem Pharmacol.* 2010; 79:154–161. [PubMed: 19720054]
18. Chen ZS, Aoki S, Komatsu M, et al. Reversal of drug resistance mediated by multidrug resistance protein (MRP) 1 by dual effects of agosterol A on MRP1 function. *Int J Cancer.* 2001; 93:107–113. [PubMed: 11391629]
19. Izumchenko E, Singh MK, Plotnikova OV, et al. NEDD9 promotes oncogenic signaling in mammary tumor development. *Cancer Res.* 2009; 69:7198–7206. [PubMed: 19738060]

20. Takayanagi S, Kataoka T, Ohara O, Oishi M, Kuo MT, Ishikawa T. Human ATP-binding cassette transporter ABCC10: expression profile and p53-dependent upregulation. *J Exp Ther Oncol*. 2004; 4:239–246. [PubMed: 15724843]
21. Oguri T, Ozasa H, Uemura T, et al. MRP7/ABCC10 expression is a predictive biomarker for the resistance to paclitaxel in non-small cell lung cancer. *Mol Cancer Ther*. 2008; 7:1150–1155. [PubMed: 18445659]
22. Bessho Y, Oguri T, Ozasa H, et al. ABCC10/MRP7 is associated with vinorelbine resistance in non-small cell lung cancer. *Oncol Rep*. 2009; 21:263–268. [PubMed: 19082471]
23. Naramoto H, Uematsu T, Uchihashi T, et al. Multidrug resistance -associated protein 7 expression is involved in cross resistance to docetaxel in salivary gland adenocarcinoma cell lines. *International Journal of Oncology*. 2007; 30:393–401. [PubMed: 17203221]
24. Zhou Y, Hopper-Borge E, Shen T, et al. Cepharanthine is a potent reversal agent for MRP7(ABCC10)-mediated multidrug resistance. *Biochem Pharmacol*. 2009; 77:993–1001. [PubMed: 19150344]
25. Kuang YH, Shen T, Chen X, et al. Lapatinib and erlotinib are potent reversal agents for MRP7 (ABCC10)-mediated multidrug resistance. *Biochem Pharmacol*. 2009
26. Shen T, Kuang YH, Ashby CR, et al. Imatinib and nilotinib reverse multidrug resistance in cancer cells by inhibiting the efflux activity of the MRP7(ABCC10). *PLoS One*. 2009; 4:e7520. [PubMed: 19841739]

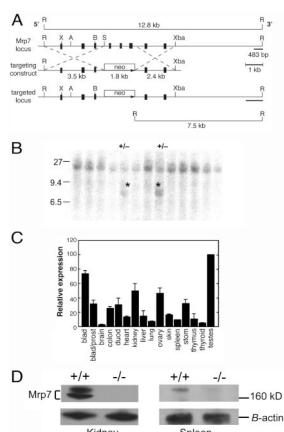


Fig. 1. Targeted disruption of the *Abcc10* gene in mice

A) Schematic of the targeting strategy. Shown are a portion of the *Abcc10* gene in which exons encoding part of nucleotide binding domain-1 reside, the targeting construct, the predicted targeted locus and endonuclease restriction sites, predicted EcoRI fragments for the wild-type and targeted locus (top and bottom, respectively) and location of the 3' probe used for Southern blot analysis. The targeting construct is designed to delete exons 6 – 8 (amino acids 204–332), which include the coding sequence of the entire Walker B motif required for ATPase activity, and to cause a frameshift which results in a prematurely terminated *Abcc10* protein. Proper recombination replaces 2.3 kb of *Abcc10* sequence with the 1.8 kb neomycin cassette and introduces an EcoRI site. Exons are shown as black rectangles. **B)** Southern blot analysis of EcoRI-digested DNA prepared from representative ES cell clones. Wild-type restriction fragments (12 kb) are seen in all lanes, and the 7.5-kb fragment (indicated by *) resulting from proper recombination are found in the 2 lanes labeled +/- . **C)** Relative expression levels of *Abcc10* mRNA in mouse tissues as assessed by real-time Taqman PCR assay. Values are averages and SD's of two reactions with different amounts of RNA. Data are presented using an arbitrary scale with mRNA levels in testes set to 100. For each sample, the values are average and standard deviation of data from two PCR reactions performed with two amounts of total RNA (50 ng and 12.5 ng) in the RT reaction. **D)** Immunoblot detection of *Abcc10* in primary kidney cell lines and spleen. Fifty micrograms of kidney cellular lysate and 20 μ g of spleen membranes were analyzed. *Abcc10* is indicated by the bracket and a molecular weight marker is shown to the right

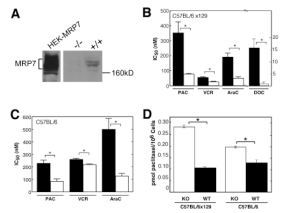


Fig. 2. Drug resistance analysis of *Abcc10*^{-/-} mouse embryo fibroblasts

A) Analysis of *Abcc10* protein expressed in MEFs. Membranes (20 μ g) prepared from wild-type (WT103.2) and *Abcc10* null mice (KO95.2) were separated by SDS-PAGE and analyzed with *Abcc10* antibody. The positive control (left) is ABCC10-transfected HEK293 cells (20 μ g). **B), C)** Drug sensitivity of *Abcc10* null and wild-type MEFs to various agents. MEFs generated from C57BL/6x129 (B) and C57BL/6 (C) wild-type and *Abcc10* null mice were analyzed for sensitivity to the indicated agents using an MTS/PMS assay. In B, the cell lines are WT103.2 (wild-type) and KO95.2 (knock out); in C, WT3-3 (wild-type) and BK07 (knockout). **D)** Accumulation of paclitaxel in wild-type (WT103.2) and *Abcc10*^{-/-} (KO95.2) MEFs. Cells (C57BL/6x129 - WT103.2, KO95.2; C57BL/6 - WT3-3, BK07) were incubated in the presence of 0.1 μ M [³H]paclitaxel and accumulation was measured at 30 minutes. Data are means \pm SDs. B - C, * $P < 0.05$ as assessed by the Two-tailed Wilcoxon test. *;D, $P < 0.05$ as assessed by the Wilcoxon two sided, two sample test.

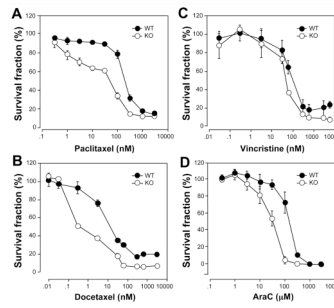


Fig. 3. Drug sensitivity curves for wild type and *Abcc10*^{-/-} MEFs

A) paclitaxel, **B)** docetaxel, **C)** vincristine, **D)** Ara-C. Representative drug sensitivity curves are shown for wild-type (WT103.2, closed symbols) and *Abcc10*^{-/-} (KO95.2, open symbols) MEFs. Data points are means \pm SDs of triplicate determinations. Representative experiments are shown.

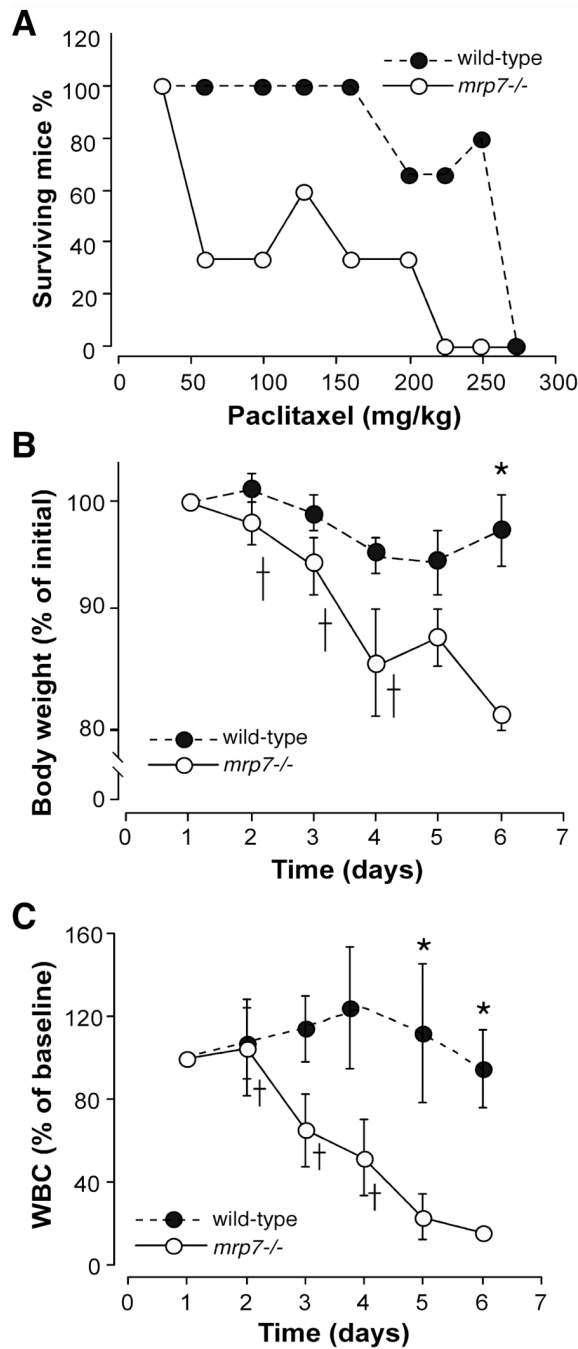


Fig. 4. Toxicity of paclitaxel in wild type and *Abcc10*^{-/-} mice

A Survival of wild-type and *Abcc10*^{-/-} mice treated with paclitaxel. Female mice (C57BL/6x129; n = 8) were treated with a range of paclitaxel dosages administered as a single intraperitoneal injection. $P < 0.005$, logistic regression. **B, C**, Analysis of white blood cell counts and body weight. Female mice (n = 5) were treated with a single 20 mg/kg dose of paclitaxel administered by intraperitoneal injection and measurements of white blood cell counts B and body weight C were made over a 6-day time course. *, $P < 0.05$ Wilcoxin one sided test; †, death.

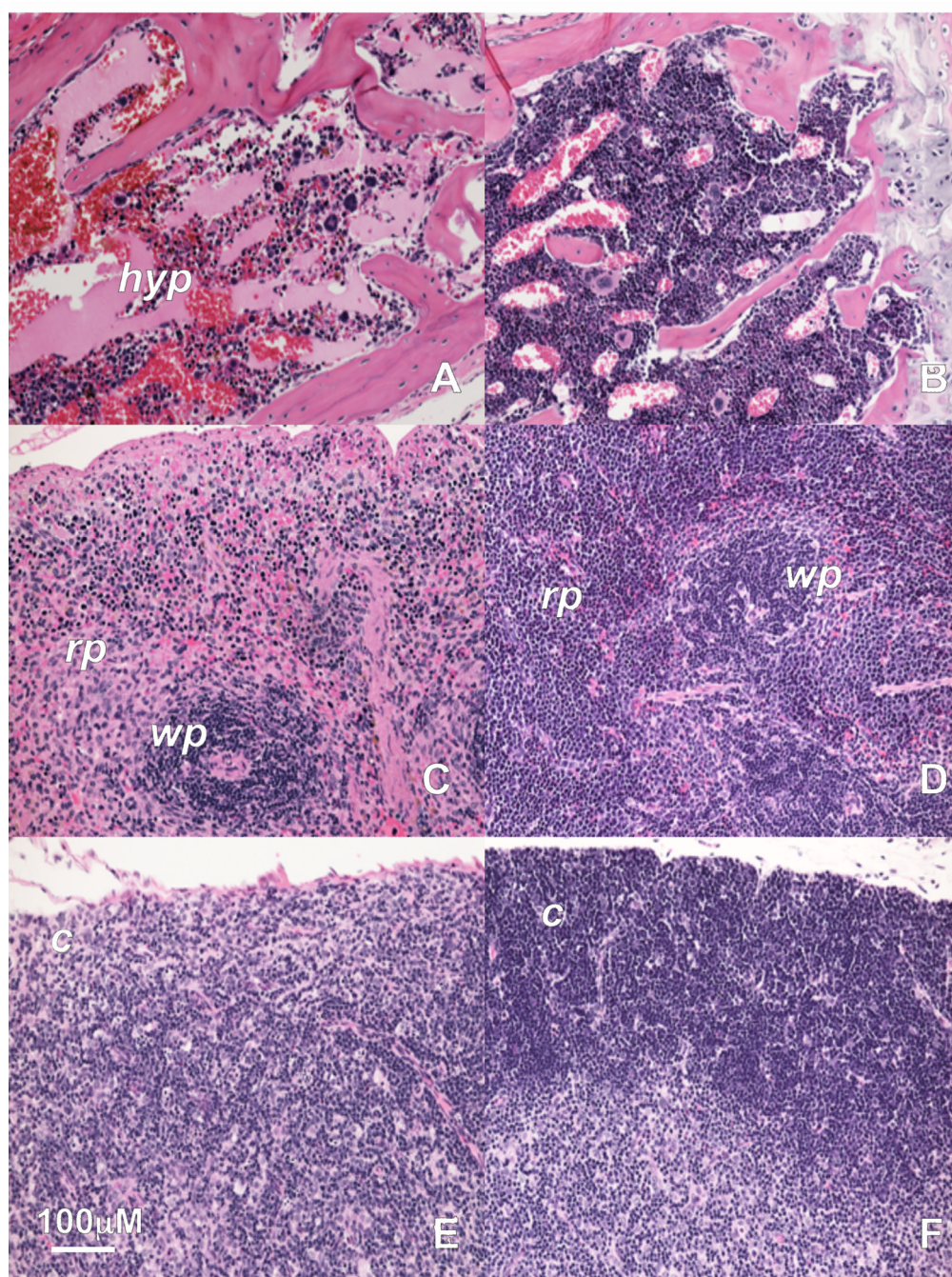


Fig. 5. Histopathologic analysis of bone marrow, spleen and thymus

A,B, bone marrow, **C,D** spleen, and **E,F** thymus. *Abcc10*^{-/-} mice (left panels); wild-type mice (right panels). Mice were treated with 20 mg/kg paclitaxel administered as a single intraperitoneal injection to wild-type and *Abcc10*^{-/-} mice, and histopathologic analysis was performed at time of death or on day 6; *c*, cortical region. *rp*, red pulp; *wp*, white pulp; *hyp*, hypoplasia; Original magnification X80Bar= 100 microns